Structural Rationale for the Coupled Binding and Unfolding of the c-Myc Oncoprotein by Small Molecules

Ariele Viacava Follis,[1] Dalia I. Hammoudeh,[1] Huabo Wang,[2] Edward V. Prochownik,[2,3,4] and Steven J. Metallo[1,*]

[1]Department of Chemistry, Georgetown University, Washington, DC 20057, USA
[2]Section of Hematology/Oncology, Children's Hospital of Pittsburgh, Pittsburgh, PA 15213, USA
[3]The University of Pittsburgh Cancer Institute, Pittsburgh, PA 15232, USA
[4]Department of Microbiology and Molecular Genetics, University of Pittsburgh Medical Center, Pittsburgh, PA 15213, USA
*Correspondence: sjm24@georgetown.edu

SUMMARY

The basic-helix-loop-helix-leucine-zipper domains of the c-Myc oncoprotein and its obligate partner Max are intrinsically disordered (ID) monomers that undergo coupled folding and binding upon heterodimerization. We have identified the binding sites and determined the structural means by which two unrelated small molecules, 10058-F4 and 10074-G5, bind c-Myc and stabilize the ID monomer over the highly ordered c-Myc-Max heterodimer. In solution, the molecules bind to distinct regions of c-Myc and thus limit its ability to interact with Max and assume a more rigid and defined conformation. The identification of multiple, specific binding sites on an ID domain suggests that small molecules may provide a general means for manipulating the structure and function of ID proteins, such as c-Myc.

INTRODUCTION

Natively unstructured or intrinsically disorderd (ID) proteins are widespread and prevalent in eukaryotes. These proteins may be unstructured throughout their entire length or contain substantial ID segments (Oldfield et al., 2005; Uversky, 2002; Wright and Dyson, 1999). Of the proteins possessing such ID sequences, those involved in cell signaling and gene regulation are overrepresented; moreover, approximately 60% of human cancer-associated proteins are predicted to have unstructured regions of $\geq$50 consecutive residues (Iakoucheva et al., 2002). Disordered regions are frequently involved in protein-protein or protein-nucleic acid interactions, and these interactions are often accompanied by a folding transition of the disordered region; that is, they undergo coupled folding and binding (Dyson and Wright, 2002). The extended nature of disordered regions, and the consequent solvent-exposed surface area, allows them to form large interfaces efficiently (Gunasekaran et al., 2003). Energetically, the coupling of folding to binding results in very specific but comparatively weak interactions: only the correct partner that provides the needed complementary surface generates sufficient enthalpic gain to compensate for the loss of entropy upon folding (Dyson and Wright, 2005).

The oncogenic transcription factor c-Myc regulates many important cellular processes, and overexpression of c-Myc occurs in many human cancers (Dang, 1999; Ponzielli et al., 2005). c-Myc heterodimerizes with a partner protein, Max, via the association of basic-helix-loop-helix-leucine-zipper (bHLHZip) domains found in both proteins (Blackwood and Eisenman, 1991). As a result of this interaction, which is required for all known biological effects of c-Myc, specific DNA binding and target gene regulation is achieved (Dang, 1999; Ponzielli et al., 2005). While the c-Myc bHLHZip domain is predominantly α helical in its dimeric form, the monomeric form is disordered (Nair and Burley, 2003). Several groups have identified compounds that can disrupt c-Myc and Max interaction (c-Myc inhibitors) (Berg et al., 2002; Kiessling et al., 2006; Xu et al., 2006; Yin et al., 2003). However, the specific protein sites to which they bind and the precise means by which heterodimerization is abrogated have not been defined.

Previously, we demonstrated that one of these compounds binds exclusively to the ID monomeric c-Myc bHLHZip domain and not at all to the bHLHZip domain of Max (Wang et al., 2007). Such an interaction implies a mechanism in which specific binding is coupled to *unfolding* of the target protein, a mode of action different from that of other described inhibitors of protein-protein interactions (Arkin and Wells, 2004). Understanding the basis for ID binding by small molecules could lead to a more general approach to the chemical modulation of protein interactions characterized by coupled folding and binding (Dyson and Wright, 2002). In addition, it could significantly enhance the development of binding molecules, as well as the ability to predict binding sites on ID proteins. Their overrepresentation in multiple diseases and as hubs in eukaryotic signaling and regulation networks makes ID proteins of increasing interest as targets; however, we are just beginning to understand how small molecules may interact with these proteins (Uversky et al., 2008).

RESULTS AND DISCUSSION

All previously described c-Myc inhibitors were found by screening for disruption of the c-Myc-Max interaction without knowledge of where on the sequence the molecules bound. For protein-protein interactions in which a separated partner retains its structure (even if the other partner does not), small-molecule binding sites may be predicted by examining the exposed interaction surface (Arkin and Wells, 2004). In contrast, the entire ID
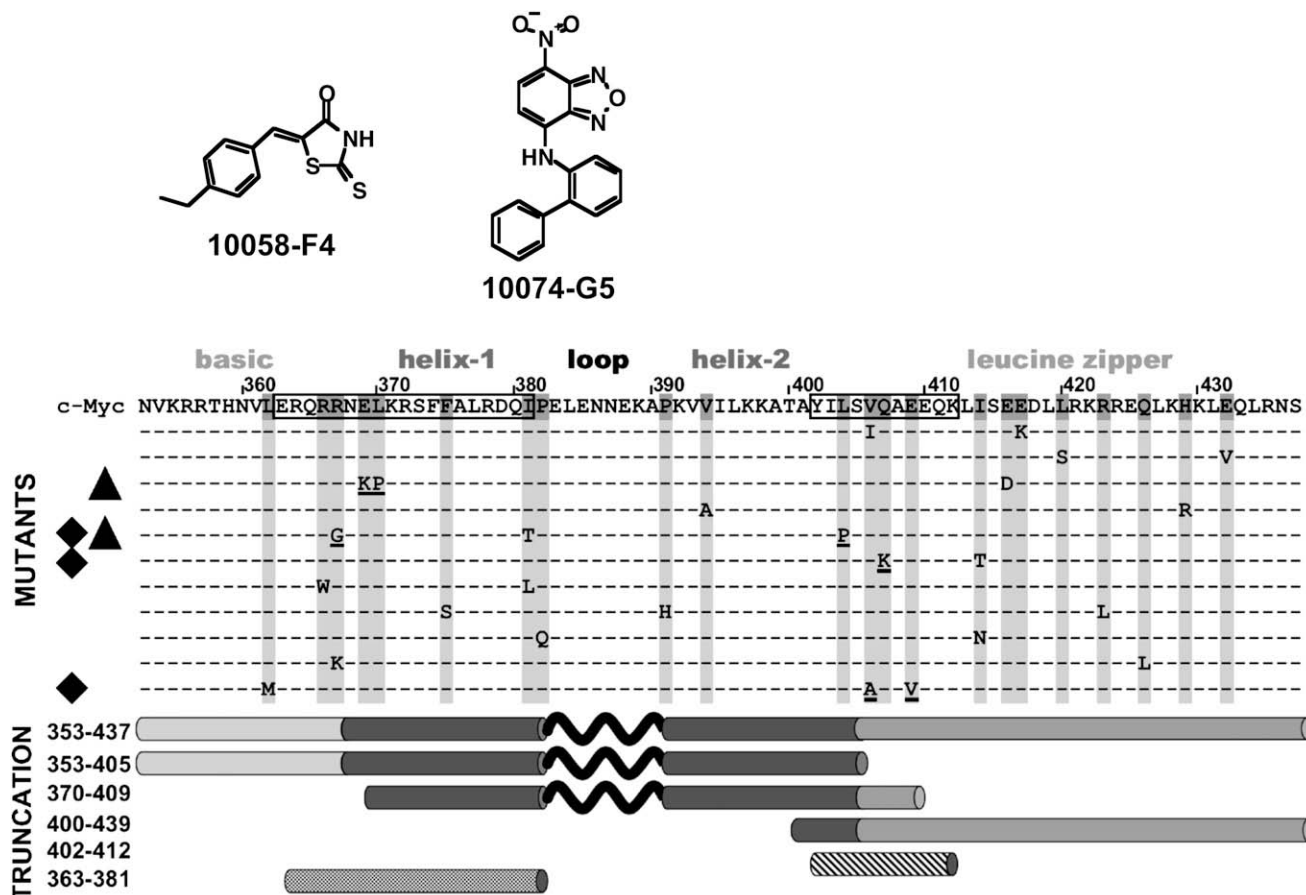
Figure 1. Scheme of c-Myc bHLHZip Mutations and Truncations Employed to Determine the Inhibitors' Binding Sites
Mutants that altered c-Myc affinity for 10058-F4 (diamonds) or 10074-G5 (triangles) are indicated; the other mutations did not have substantial effects on binding.

sequence of the c-Myc HLHZip domain (both residues that contact Max in the dimer and those that do not) has the potential to act as a binding site. In addition, the conformation of c-Myc in its heterodimeric form does not provide any insight as to potential compound binding sites in the ID monomer. To begin to understand the basis for this atypical inhibition, we first located binding sites for two compounds on the c-Myc bHLHZip sequence. These molecules, 10058-F4 and 10074-G5 (Yin et al., 2003), which exhibit intrinsic fluorescence, were exploited in a fluorescence polarization assay to monitor direct binding to purified recombinant c-Myc bHLHZip domain (c-Myc$_{353–437}$). Initial experiments indicated that 10058-F4 and 10074-G5 bound c-Myc$_{353–437}$ with 5.3 ± 0.7 μM and 2.8 ± 0.7 μM affinities, respectively, and with 1:1 stoichiometry. The compounds bound to c-Myc simultaneously and independently, indicating that each binding site within the bHLHZip sequence was unique and distinct (Figure S1).

We next generated a series of c-Myc bHLHZip point mutants and truncations in order to map the inhibitors' binding sites (Figure 1). Binding of 10058-F4 was impaired by the mutation of residues at the interface between helix 2 and the leucine zipper (L$_{404}$P, Q$_{407}$K, and V$_{406}$A–E$_{409}$V) and by deletion of the leucine zipper region (c-Myc$_{353–405}$). In contrast, binding of 10074-G5

was actually enhanced by mutations between the basic region and helix 1 (R$_{367}$G and E$_{369}$K–L$_{370}$P) and eliminated in truncations c-Myc$_{370–409}$ and c-Myc$_{400–439}$. Next, two peptides were synthesized, c-Myc$_{402–412}$ and c-Myc$_{363–381}$, each encompassing only a single deduced binding site. These peptides bound 10058-F4 and 10074-G5, with K$_D$ = 13 ± 1 μM and K$_D$ = 4.4 ± 0.8 μM, respectively—values close to those observed for full-length c-Myc$_{353–437}$ (Figure S1). Since c-Myc$_{353–437}$ and the peptides derived from it lack stable structure, the binding observed was dictated solely by a short segment of the primary sequence. The dependence only on primary sequence implies that a rational, sequence-based approach to the search for binding sites in other ID proteins may be possible.

Upon binding either 10058-F4 or 10074-G5, the circular dichroism (CD) spectra of the full-length c-Myc bHLHZip domain displayed only minor changes (Figure 2A). These results indicate that this domain retained its predominantly disordered structure even after complex formation, and suggest that any alterations in protein conformation were probably localized to short regions around the binding sites. To make any such localized structural rearrangements more apparent, the peptides c-Myc$_{363–381}$ and c-Myc$_{402–412}$ were examined. The CD spectrum of each short peptide was markedly altered by the binding of its cognate
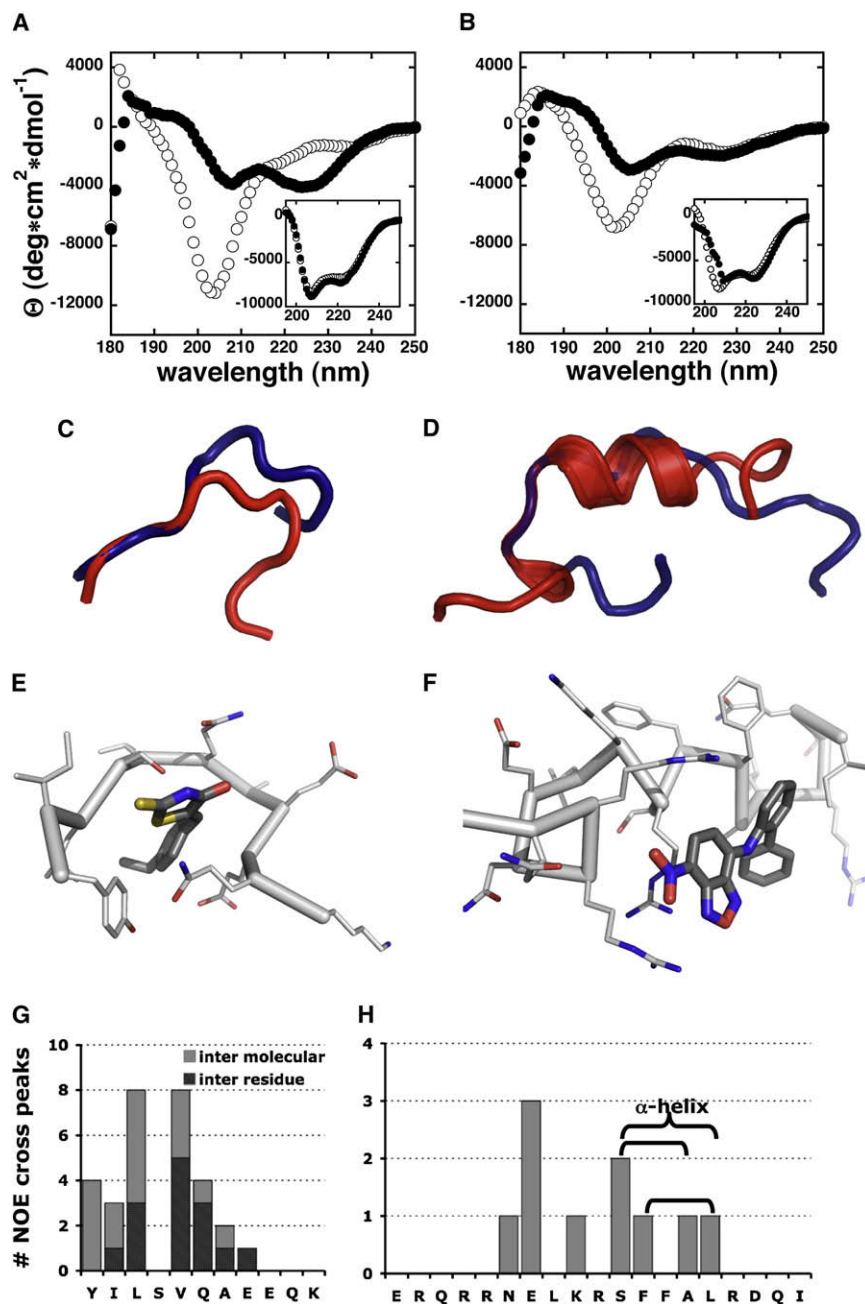
Figure 2. Small Molecules Induce Conformational Changes in Target Peptides

(A) CD spectra of 20 μM c-Myc$_{402-412}$ in the absence (white circles) and presence (black circles) of an equimolar amount of 10058-F4.

(B) CD spectra of 20 μM c-Myc$_{363-381}$ in the absence (white circles) and presence (black circles) of 10074-G5. Insets show the spectra of 10 μM c-Myc$_{353-437}$ in the absence and presence of an equimolar amount of each inhibitor.

(C) Overlaid models of c-Myc$_{402-412}$ in the free (blue) and bound (red) states. The models represent a likely average conformation of the dynamic ensemble constituting each state.

(D) Free and bound models of c-Myc$_{363-381}$.

(E) Docking between 10058-F4 and c-Myc$_{402-412}$.

(F) Docking between 10074-G5 and c-Myc$_{363-381}$.

(G) Sequence distribution of side chain NOESY cross peaks observed in the c-Myc$_{402-412}$-10058-F4 complex.

(H) Analogous plot for the c-Myc$_{363-381}$-10074-G5 complex. Ambiguously assigned cross peaks and ones between adjacent residues are omitted. Neither free peptide displayed any NOESY cross-peaks between nonadjacent residues.

differences in ^{1}H and ^{13}C chemical shifts for four backbone and several side chain signals upon addition of 10058-F4 (Figures S4 and S5). The splitting observed for Tyr$_{402}$ β peaks indicated that complex formation induced these protons to become diastereotopic. The ^{1}H aromatic signals of Tyr$_{402}$ shifted upfield upon complex formation in both c-Myc$_{402-412}$ and full-length c-Myc$_{353-437}$, yet this ring, and the 10058-F4 aromatic moiety, were rotationally unconstrained. Strong quenching (80%) and a blue shift (302–296 nm) in the emission maximum of the Tyr$_{402}$ fluorescence in the 10058-F4 complex with either c-Myc$_{402-412}$ or c-Myc$_{353-437}$ indicated proximity between the aromatic moieties of the peptide and inhibitor and a change in the surroundings of the tyrosine (Lee and Ross, 1998). Partial backbone assignments for ^{1}H spectra of c-Myc$_{353-437}$ allowed identification of corresponding changes to those observed in c-Myc$_{402-412}$ upon complex formation. A change in shift and shape of the aromatic signals of 10074-G5 was also observed in this case, possibly due to its increased segregation from the solution environment. The similar behaviors of the minimal c-Myc$_{402-412}$ peptide and the larger c-Myc$_{353-437}$ bHLHZip domain confirmed that the binding interaction with 10058-F4 caused only local perturbations around residues 402–412, and that flanking residues remained largely unaffected. The NOESY spectrum of the c-Myc$_{402-412}$-10058-F4 complex displayed 16 intermolecular and 7 interresidue cross peaks (none of which are present in the NOESY spectrum of the free peptide), involving residues located at the N terminus of the

compound, as indicated by the disappearance of a minimum at 207 nm, typical of random coil features (Figures 2A and 2B). The highly localized nature of these binding sites, and hence the localization of any conformational restrictions coupled to binding, could grant an entropic advantage to small, c-Myc binding molecules: the affinity of 10058-F4 for c-Myc is only ∼1.6 kcal mol^{-1} lower than that of Max, despite a greater than 10-fold difference in interaction surface areas (10058-F4 area: 275 Å^2; c-Myc-Max interface: 3206 Å^2 [Nair and Burley, 2003]).

To characterize structural features of the individual complexes, the peptides encompassing the two binding sites (c-Myc$_{402-412}$, c-Myc$_{363-381}$) were studied by ^{1}H and ^{13}C NMR in the absence and presence of inhibitor. The spectra of c-Myc$_{402-412}$ displayed

peptide. These cross peaks indicated the formation of a hydrophobic cluster comprised of side chains from Tyr_{402}, Ile_{403}, Leu_{404}, Val_{406}, Ala_{408}, and the aromatic ring of the inhibitor and its ethyl moiety (Figure S6). The weak intensity and low number of cross peaks are due to the intermediate relaxation time range of the small peptide. The paucity of NOESY signals from the C terminus suggests higher mobility in solution than the N-terminal residues.

NMR analysis of complex formation between 10074-G5 and c-$Myc_{363-381}$ showed changes in the chemical shift of 10 Hα, 11 Cα signals, and the terminal side chain resonance of two Arg residues (Figures S7 and S8). The larger number of backbone chemical shift differences in the 10074-G5 complex indicated that more residues underwent a conformational change in this complex. A convergence to ~7.4 ppm of the ^{1}H shifts of the inhibitors' heteroaromatic moiety, observed at ~7.9 and ~6.2 ppm in the free compound, showed an altered chemical environment for this ring. The NOESY spectrum of the complex showed 25 interresidue cross peaks, which were absent in the free peptide, including a pattern of signals between residues three positions away indicating an α-helical conformation within Leu_{370}–Leu_{377}. No NOESY cross peaks between nonadjacent residues were observed in the free peptide. The signal overlap between the aromatic signals of phenylalanine residues and inhibitor prevented the unambiguous assignment of intermolecular cross peaks (Figure S9).

Secondary structure trends of c-$Myc_{402-412}$ and c-$Myc_{363-381}$ in their free and bound states were assessed by means of ^{1}Hα and ^{13}Cα chemical shift indexing (Wishart et al., 1992): peaks affected by complex formation moved further from random coil values in the same direction of the field as observed for their shift in the unbound state (Figures S5 and S8). Such observations suggest a correspondence between the average conformation of the highly dynamic free peptide and the more rigid bound state, possibly related to the presence of local conformational constraints in the free peptide (Barre and Eliezer, 2006; Rose et al., 2006). Due to the limited NOESY information, it was not possible to effectively employ distance constraints to generate NMR structures; instead, models of the peptides in their free and bound states were obtained using chemical shift-based dihedral constraints (Berjanskii et al., 2006). A docking simulation was then performed between the bound structures and respective inhibitors, with the resulting models intended to represent one reasonable conformation out of the likely dynamic ensemble constituting each complex (Figures 2C–2F). In neither complex did the peptide conformation correspond to that found in the c-Myc-Max crystal structure, thus clearly demonstrating that the product of a coupled folding and binding reaction may not be useful in predicting potential small-molecule binding sites or their conformations. Furthermore, the conformations of the peptides in the bound form appear incompatible with formation of the HLHZip interface and provide a rationale for dimer inhibition. The comparison of the free and bound models indicated the formation of a pocket upon complex formation in both peptides. In the c-$Myc_{402-412}$-10058-F4 docking, the inhibitor was located at the center of a C-shaped cavity, in an orientation that allowed for hydrophobic interactions to take place between its aromatic ring and ethyl tail and the peptides N-terminal hydrophobic side chains. The carbonyl oxygen of 10058-F4 was within hydro-

gen-bonding range with Ser_{406} and Gln_{407} side chains. Although generated independently, this model matched the NOESY indication of hydrophobic interactions (Figure 2G). The docking between c-$Myc_{363-381}$ and 10074-G5 displayed the inhibitor enclosed in a cavity generated by a kink at the N terminus of a helical segment spanning from Leu_{370} to Arg_{378}, its biphenyl moiety close to the aromatic ring of Phe_{375}, and the electron-rich heteroaromatic and nitro moieties interacting with the positively charged $Arg_{366-367}$. This model also agreed with the independent NOESY results, which indicate the induction of a helical segment upon complex formation (Figure 2H).

The inhibitory effects of 10058-F4 and 10074-G5 on c-Myc bHLHZip functionality were then tested in vitro. Alone, c-$Myc_{353-437}$ displayed a CD signal typical of disordered protein regions (Tompa, 2002). Heterodimers were formed between the c-Myc bHLHZip and Max(p21), a Max isoform with low homodimer affinity, but strong heterodimer affinity (K_D^{dimer} = 0.43 ± 0.02 μM). The heterodimer complex displayed a characteristic α-helical CD curve expected from the complete folding of the HLHZip domain. Addition of the inhibitors confirmed their ability to disrupt heterodimer formation and induce unfolding of the complex. The addition of 10058-F4 to the heterodimer led to complete disordering of c-Myc and Max. The competition constant (the ratio of c-Myc-inhibitor K_D to c-Myc-Max K_D, as measured by competition) between 10058-F4 and Max(p21) was 12.4 ± 0.4—very close to the ratio (12.3) between the independently determined c-Myc binding affinities. The addition of 10074-G5 also strongly disrupted the complex, although not to the same extent as 10058-F4. The higher-than-predicted competition constant between 10074-G5 and Max(p21) (37 ± 2 versus an independent K_D ratio of 6.7) and an increased helical content at the titration endpoint indicate lower efficacy of this inhibitor in disrupting c-Myc-Max complexes (Figures 3B and 3C). This observation may be explained by the position of 10074-G5's interaction site, which lies at the extreme edge of the c-Myc dimerization interface. Some residual associations between the leucine zipper regions, located at the opposite end of the domain, may still be possible in the presence of 10074-G5.

The finding of two independent binding sites, each comprised of about 10 residues within an 84 amino acid-long bHLHZip domain, may indicate that sites capable of specific small-molecule binding are widespread in ID proteins. The ability of small molecules to bind with high specificity to nontraditional, flexible binding sites within the context of a family of conserved proteins led us to examine potential determinants of specificity in the c-Myc sequence. The bHLHZip domains of Max and Mad member proteins, the binding of which was not disrupted by 10058-F4 or 10074-G5 (based on the original screening [Yin et al., 2003]) were therefore compared with c-Myc. An unusually high level of residues conserved among Max and Mad proteins, but not conserved in c-Myc, was found in the two binding segments. Out of 22 such nonconserved residues scattered throughout the c-$Myc_{353-437}$ sequence, five occurred within the 10058-F4 binding segment (Leu_{404}–Ala_{408}) and another four occurred within the 10074-G5 binding site (Asn_{369}, Leu_{370}, Phe_{375}, and Ala_{376}) (Figure S10). Furthermore, these regions contain two of the three clusters of four hydrophobic residues found in the c-Myc bHLHZip, and these regions are more hydrophobic than
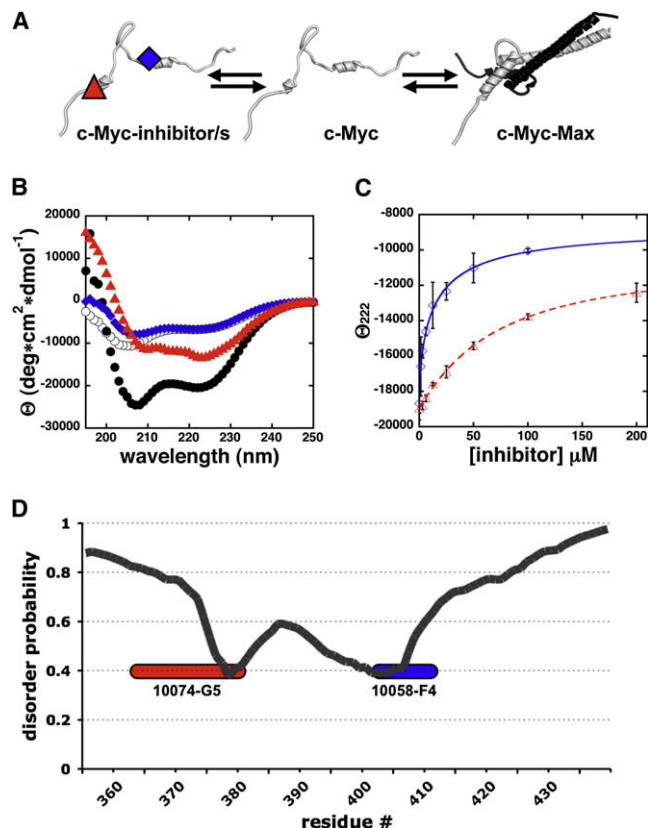
Figure 3. Disruption of Myc-Max Dimer

(A) Schematic representation of the competition for c-Myc binding. The inhibitors' binding stabilizes the globally disordered state of c-Myc and Max monomers.

(B) Weighted average of the independently recorded CD spectra of 10 μM c-Myc$_{353-437}$ and 10 μM Max(p21) (white circles), 1:1 mixture of c-Myc$_{353-437}$-Max(p21) in the absence (black circles) and presence of 200 μM 10058-F4 (blue diamonds) or 10074-G5 (red triangles).

(C) Competition between 10058-F4 (blue diamonds) or 10074-G5 (red triangles) and Max(p21). Increasing inhibitor concentrations were incubated with a 1.5 μM 1:1 mixture of c-Myc$_{353-437}$ and Max(p21). The competition constant used to generate the competition curve fit corresponds to the ratio of the Myc affinity $K_D^{inhibitor}/K_D^{dimer}$. Error bars represent SEM.

(D) Output of the disorder predictor PONDR VSL2B for c-Myc$_{353-437}$. Positions of binding site containing peptides are overlaid and occur in regions of transition from high to low predicted disorder.

the corresponding sequences of other bHLHZip proteins. Analysis of the c-Myc bHLHZip sequence with the disorder-predicting algorithm PONDR (Obradovic et al., 2005) indicates two regions with abrupt changes in disorder probability that overlap the experimentally determined binding sites (Figure 3D). In searching for potential binding sites of small molecules on ID proteins, in which such sites may be located anywhere along the sequence, identification of regions of predicted low disorder that also contain nonconserved residues may indicate sequences that are capable both of binding and of specificity. High hydrophobic content and low disorder probability are sequence properties also observed for ID protein regions involved in recognition of protein partners (molecular recognition elements) (Uversky et al., 2005). ID proteins are able to adopt alternate conformations in complex with different protein partners (Tompa et al., 2005).

Similarly, Max induces one structure in the bHLHZip of Myc, while the small molecules induce alternate, localized structures.

Other examples exist of binding interactions between proteins and small molecules, the selectivity of which depends on short peptide sequences (Rodi et al., 1999). Morohashi et al. (2005) defined short peptides capable of binding the small-molecule NK109 as "drug target motifs." Recently, small molecules were found that act as substrate-targeted inhibitors (Kodadek, 2002), which bind a short hydrophobic sequence on β-amyloid precursor protein (Kukar et al., 2008).

The structured interaction partners of ID proteins have been proposed as drug targets (Cheng et al., 2006). The potential wide-spread existence of ID protein segments susceptible to small-molecule binding also suggests the possibility of specific chemical modulation of ID proteins by targeting the ID proteins themselves. Interactions between ID proteins tend to be optimized for functional flexibility, having relatively low affinity yet high specificity due to the entropy loss related to the structural induction required by complex formation (Dyson and Wright, 2005). Interactions akin to those described here, with affinities in the low micromolar range, might affect protein function in vivo, provided a sufficient binding specificity. Also, since more than one binding site may be found within a domain of interest, linked compounds could potentially exploit the effects of multivalency to increase both affinity and specificity. The effective targeting of ID proteins offers the potential for introducing a whole class of heretofore underappreciated targets for chemical biology and drug development.

SIGNIFICANCE

Several small molecules have been described that disrupt c-Myc-Max heterodimerization. In order to do so, these molecules specifically bind c-Myc and stabilize the intrinsically disordered (ID) monomer over the highly ordered c-Myc-Max heterodimer. The sequences and characteristics of sites within an ID region capable of specific binding by small molecules were unknown. Here, we characterize the distinct binding sites and interactions of two small molecules that form soluble, reversible complexes with c-Myc. The binding of these molecules induced a global conformational disordering that affected a protein-protein interaction occurring over a large surface area. Within a relatively short ID domain, two independent, specific binding sites were found, suggesting that potential binding sites may be prevalent in ID proteins and that the discovery of small molecules capable of modulating the conformation and interaction of various ID proteins may be practicable. The absence of protein order in ID domains with their characteristic sequence accessibility and lack of tertiary contacts, and the short, linear sites to which the current compounds have been shown to bind, further suggest that it may be possible to predict from primary amino acid sequence locations within these domains which are susceptible to specific small-molecule binding.

EXPERIMENTAL PROCEDURES

Detailed Supplemental Experimental Procedures are available online in the Supplemental Data.

Mutagenesis

The region encoding human c-Myc amino acids 351–439 was amplified via PCR with a GeneMorph II Random Mutagenesis Kit (Stratagene, Inc.), introducing an average of two point mutations/molecule, and directionally cloned into the pQE9 vector (QIAGEN, Inc.). For truncation mutagenesis, the indicated regions were amplified and directionally cloned into the pET151D vector using the TOPO ligation system (Invitrogen). Proteins were overexpressed in *Escherichia coli* BL21DE3(pLysS) cells and purified by Ni-affinity chromatography followed by reversed-phase HPLC.

Fluorescence Polarization

Inhibitors were titrated in the presence and absence of equimolar protein component. For the point mutants, the buffer contained 20 mM MES, pH 5.3, 1 mM DTT, and 5% DMSO (these proteins contain a His tag and have reduced solubility at higher pH). For all other proteins and peptides, experiments were conducted in buffer containing 1× PBS (137 mM NaCl, 2.7 mM KCl, 4.3 mM Na_2HPO_4, 1.4 mM KH_2PO_4, pH = 7.4), 1 mM DTT, and 5% DMSO. Polarization measurements were made using excitation and emission wavelengths of 380 and 468 nm, respectively, for 10058-F4, or 470 and 550 nm for 10074-G5 at 25°C, with sample specific G-factor determination and background correction. All measurements represent the average of at least three independent trials.

NMR Spectroscopy

Peptide samples (~200 to ~500 μM) in the absence or presence of inhibitor were prepared in 100% D_2O, 5 mM sodium phosphate buffer, pH 7.5, or 90% H_2O-10% D_2O, 5 mM sodium phosphate buffer, pH 6.3 (for $H_α(i)$–$H_N(i + 1)$ NOE sequential assignments). Two-dimensional ^1H homonuclear and ^1H-^{13}C HMQC spectra were recorded at 25°C over sweep widths of ~10 × 10 ppm (~140 × 10 ^{13}C) with 16–64 scans/t_1 increment, 1.5–2 s relaxation delay, and sizes of 512–1024 × 2048 complex points. NOE mixing times of 300, 250, and 150 ms were employed for c-$Myc_{402-412}$, c-$Myc_{363-381}$, and c-$Myc_{353-437}$, respectively.

Molecular Modeling

Peptide models generated from PREDITOR (Berjanskii et al., 2006) dihedral constraints were energy minimized using CHARMM27 parameters (MacKerell et al., 1998). The inhibitors were flexibly docked to the bound conformation model of their respective binding sites using the AutoDock LGA algorithm (Morris et al., 1998).

SUPPLEMENTAL DATA

Supplemental Data include Supplemental Experimental Procedures, Supplemental References, ten figures, and five tables and can be found with this article online at http://www.chembiol.com/cgi/content/full/15/11/1149/DC1/.

REFERENCES

Arkin, M.R., and Wells, J.A. (2004). Small-molecule inhibitors of protein-protein interactions: progressing towards the dream. Nat. Rev. Drug Discov. *3*, 301–317.

Barre, P., and Eliezer, D. (2006). Folding of the repeat domain of tau upon binding to lipid surfaces. J. Mol. Biol. *362*, 312–326.

Berg, T., Cohen, S.B., Desharnais, J., Sonderegger, C., Maslyar, D.J., Goldberg, J., Boger, D.L., and Vogt, P.K. (2002). Small-molecule antagonists of Myc/Max dimerization inhibit Myc-induced transformation of chicken embryo fibroblasts. Proc. Natl. Acad. Sci. USA *99*, 3830–3835.

Berjanskii, M.V., Neal, S., and Wishart, D.S. (2006). PREDITOR: a web server for predicting protein torsion angle restraints. Nucleic Acids Res. *34*, W63–W69.

Blackwood, E.M., and Eisenman, R.N. (1991). Max: a helix-loop-helix zipper protein that forms a sequence-specific DNA-binding complex with Myc. Science *251*, 1211–1217.

Cheng, Y., LeGall, T., Oldfield, C.J., Mueller, J.P., Van, Y.Y., Romero, P., Cortese, M.S., Uversky, V.N., and Dunker, A.K. (2006). Rational drug design via intrinsically disordered protein. Trends Biotechnol. *24*, 435–442.

Dang, C.V. (1999). c-Myc target genes involved in cell growth, apoptosis, and metabolism. Mol. Cell. Biol. *19*, 1–11.

Dyson, H.J., and Wright, P.E. (2002). Coupling of folding and binding for unstructured proteins. Curr. Opin. Struct. Biol. *12*, 54–60.

Dyson, H.J., and Wright, P.E. (2005). Intrinsically unstructured proteins and their functions. Nat. Rev. Mol. Cell Biol. *6*, 197–208.

Gunasekaran, K., Tsai, C.J., Kumar, S., Zanuy, D., and Nussinov, R. (2003). Extended disordered proteins: targeting function with less scaffold. Trends Biochem. Sci. *28*, 81–85.

Iakoucheva, L.M., Brown, C.J., Lawson, J.D., Obradovic, Z., and Dunker, A.K. (2002). Intrinsic disorder in cell-signaling and cancer-associated proteins. J. Mol. Biol. *323*, 573–584.

Kiessling, A., Sperl, B., Hollis, A., Eick, D., and Berg, T. (2006). Selective inhibition of c-Myc/Max dimerization and DNA binding by small molecules. Chem. Biol. *13*, 745–751.

Kodadek, T. (2002). Inhibition of proteolysis and other posttranslational modifications with substrate-targeted inhibitors. Biopolymers *66*, 134–140.

Kukar, T.L., Ladd, T.B., Bann, M.A., Fraering, P.C., Narlawar, R., Maharvi, G.M., Healy, B., Chapman, R., Welzel, A.T., Price, R.W., et al. (2008). Substrate-targeting gamma-secretase modulators. Nature *453*, 925–929.

Lee, J.K., and Ross, R.T. (1998). Absorption and fluorescence of tyrosine hydrogen-bonded to amide-like ligands. J. Phys. Chem. B *102*, 4612–4618.

MacKerell, A.D., Jr., Bashford, D., Bellott, M., Dunbrack, R.L., Jr., Evanseck, J., Field, M.J., Fischer, S., Gao, J., Guo, H., Ha, S., et al. (1998). All-atom empirical potential for molecular modeling and dynamic studies of proteins. J. Phys. Chem. B *102*, 3586–3616.

Morohashi, K., Yoshino, A., Yoshimori, A., Saito, S., Tanuma, S., Sakaguchi, K., and Sugawara, F. (2005). Identification of a drug target motif: an anti-tumor drug NK109 interacts with a PNxxxxP. Biochem. Pharmacol. *70*, 37–46.

Morris, G.M., Goodsell, D.S., Halliday, R.S., Huey, R., Hart, W.E., Belew, R.K., and Olson, A.J. (1998). Automated docking using a Lamarckian genetic algorithm and an empirical binding free energy function. J. Comput. Chem. *19*, 1639–1662.

Nair, S.K., and Burley, S.K. (2003). X-ray structures of Myc-Max and Mad-Max recognizing DNA. Molecular bases of regulation by proto-oncogenic transcription factors. Cell *112*, 193–205.

Obradovic, Z., Peng, K., Vucetic, S., Radivojac, P., and Dunker, A.K. (2005). Exploiting heterogeneous sequence properties improves prediction of protein disorder. Proteins *61* (Suppl 7), 176–182.

Oldfield, C.J., Cheng, Y., Cortese, M.S., Brown, C.J., Uversky, V.N., and Dunker, A.K. (2005). Comparing and combining predictors of mostly disordered proteins. Biochemistry *44*, 1989–2000.

Ponzielli, R., Katz, S., Barsyte-Lovejoy, D., and Penn, L.Z. (2005). Cancer therapeutics: targeting the dark side of Myc. Eur. J. Cancer *41*, 2485–2501.

Rodi, D.J., Janes, R.W., Sanganee, H.J., Holton, R.A., Wallace, B.A., and Makowski, L. (1999). Screening of a library of phage-displayed peptides identifies human bcl-2 as a taxol-binding protein. J. Mol. Biol. *285*, 197–203.

Rose, G.D., Fleming, P.J., Banavar, J.R., and Maritan, A. (2006). A backbone-based theory of protein folding. Proc. Natl. Acad. Sci. USA *103*, 16623–16633.

Tompa, P. (2002). Intrinsically unstructured proteins. Trends Biochem. Sci. *27*, 527–533.

Tompa, P., Szasz, C., and Buday, L. (2005). Structural disorder throws new light on moonlighting. Trends Biochem. Sci. *30*, 484–489.

Uversky, V.N. (2002). Natively unfolded proteins: a point where biology waits for physics. Protein Sci. *11*, 739–756.

Uversky, V.N., Oldfield, C.J., and Dunker, A.K. (2005). Showing your ID: intrinsic disorder as an ID for recognition, regulation and cell signaling. J. Mol. Recognit. *18*, 343–384.

Uversky, V.N., Oldfield, C.J., and Dunker, A.K. (2008). Intrinsically disordered proteins in human diseases: introducing the D^2 concept. Annu. Rev. Biophys. *37*, 215–246.

Wang, H., Hammoudeh, D.I., Follis, A.V., Reese, B.E., Lazo, J.S., Metallo, S.J., and Prochownik, E.V. (2007). Improved low molecular weight Myc-Max inhibitors. Mol. Cancer Ther. *6*, 2399–2408.

Wishart, D.S., Sykes, B.D., and Richards, F.M. (1992). The chemical shift index: a fast and simple method for the assignment of protein secondary structure through NMR spectroscopy. Biochemistry *31*, 1647–1651.

Wright, P.E., and Dyson, H.J. (1999). Intrinsically unstructured proteins: reassessing the protein structure-function paradigm. J. Mol. Biol. *293*, 321–331.

Xu, Y., Shi, J., Yamamoto, N., Moss, J.A., Vogt, P.K., and Janda, K.D. (2006). A credit-card library approach for disrupting protein-protein interactions. Bioorg. Med. Chem. *14*, 2660–2673.

Yin, X., Giap, C., Lazo, J.S., and Prochownik, E.V. (2003). Low molecular weight inhibitors of Myc-Max interaction and function. Oncogene *22*, 6151–6159.